

Approach to Calculate the El Niño Oscillation: 8.23 Years

Huaiyang Cui

Department of Physics, Beihang University, Beijing, 102206, China

Email: hycui@buaa.edu.cn, hycui.blogspot.com

(August 7, 2022, submitted to viXra)

Abstract: In analogy with the ultimate speed c , there is an ultimate acceleration β , nobody's acceleration can exceed this limit β , in the solar system, $\beta=2.961520e+10(\text{m/s}^2)$. Because this ultimate acceleration is a large number, any effect connecting to β will become easy to test, including quantum gravity tests. In this paper, an approach is put forward to connect the ultimate acceleration with quantum theory, as an application, this relativistic model gives out the sunspot cycle to be 10.38 years due to the ultimate acceleration. The same approach is applied to the El Niño oscillation, calculating out the El Niño irregular period to be 8.23 years.

1. Introduction

In general, some quantum gravity proposals [1,2] are extremely hard to test in practice, as quantum gravitational effects are appreciable only at the Planck scale [3]. But ultimate acceleration gives another scheme to enhance the quantum gravity effects.

In analogy with the ultimate speed c , there is an ultimate acceleration β , nobody's acceleration can exceed this limit β , in the solar system, $\beta=2.961520e+10(\text{m/s}^2)$. Because this ultimate acceleration is a large number, any effect connecting to β will become easy to test, including quantum gravity tests. In this paper, an approach is put forward to connect the ultimate acceleration with quantum theory, as an application, this relativistic model gives out the sunspot cycle to be 10.38 years due to the ultimate acceleration. The same approach is applied to the Earth El Niño oscillation, calculating out the El Niño irregular period to be 8.23 years.

In 1843, German pharmacist H.S. Schwabe found that the growth and decline of sunspots had a period of about 10 years through his own observation records of sunspots for more than 20 years. In 1848, J.R. Wolf calculated the monthly sunspot relative number to 1749, thus affirming that the average cycle length of sunspot activity was 11.1 years. In 2019, there are 288 days without sunspots, and 40 consecutive days ahead. On December 25, 2019, two new sunspots appeared in the southern hemisphere of the sun, indicating the arrival of the 25th sunspot cycle, which is expected to reach its peak in July 2025. Although it is known that the cycle of sunspot activity is about 11 years, what drives this non-stop pattern is still a mystery.

2. How to connect the ultimate acceleration with quantum theory

In the relativity, the speed of light c is an ultimate speed, nobody's speed can exceed this limit c . The relativistic velocity u of a particle in the coordinate system $(x_1, x_2, x_3, x_4=ict)$ satisfies

$$u_1^2 + u_2^2 + u_3^2 + u_4^2 = -c^2 \quad (1)$$

No matter what particles (electrons, molecules, neutrons, quarks), their 4-vector velocities all have the same magnitude: $|u|=ic$. All particles gain **equality** because of the same magnitude of the 4-velocity u . The acceleration a of a particle is given by

$$a_1^2 + a_2^2 + a_3^2 = a^2; \quad (a_4 = 0; \quad \because x_4 = ict) \quad (2)$$

Assume that particles have an ultimate acceleration β as limit, no particle can exceed this acceleration limit β . Subtracting the both sides of the above equation by β^2 , we have

$$a_1^2 + a_2^2 + a_3^2 - \beta^2 = a^2 - \beta^2; \quad a_4 = 0 \quad (3)$$

It can be rewritten as

$$[a_1^2 + a_2^2 + a_3^2 + 0 + (i\beta)^2] \frac{1}{1 - a^2 / \beta^2} = -\beta^2 \quad (4)$$

Now, the particle subjects to an acceleration whose five components are specified by

$$\begin{aligned} \alpha_1 &= \frac{a_1}{\sqrt{1 - a^2 / \beta^2}}; & \alpha_2 &= \frac{a_2}{\sqrt{1 - a^2 / \beta^2}}; \\ \alpha_3 &= \frac{a_3}{\sqrt{1 - a^2 / \beta^2}}; & \alpha_4 &= 0; & \alpha_5 &= \frac{i\beta}{\sqrt{1 - a^2 / \beta^2}}; \end{aligned} \quad (5)$$

where α_5 is the newly defined acceleration in five dimensional space-time $(x_1, x_2, x_3, x_4=ict, x_5)$. Thus, we have

$$\alpha_1^2 + \alpha_2^2 + \alpha_3^2 + \alpha_4^2 + \alpha_5^2 = -\beta^2; \quad \alpha_4 = 0 \quad (6)$$

It means that the magnitude of the newly defined acceleration α for every particle takes the same value: $|\alpha|=i\beta$ (constant imaginary number), all particle accelerations gain **equality** for the sake of the same magnitude.

How to resolve the velocity u and acceleration a into x, y, z components? In realistic world, a hand can rotate a ball moving around a circular path at constant speed v with constant centripetal acceleration a , as shown in Fig.1(a).

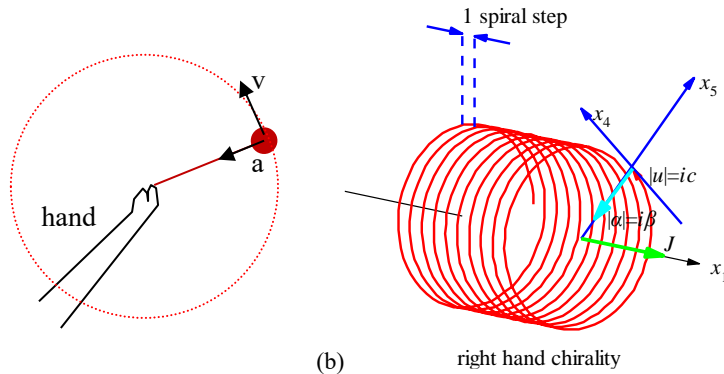


Fig.1 (a) A hand rotates a ball moving around a circular path at constant speed v with constant centripetal acceleration a . (b) The particle moves along the x_1 axis with the constant speed $|u|=ic$ in the u direction and constant centripetal force in the x_5 axis at the radius iR (imaginary number).

```
<Clet2020 Script>// Clet is a C compiler[26]
double D[100],S[2000];int i,j,R,X,N;
int main(){R=50;X=50;N=600;D[0]=-50;D[1]=0;D[2]=0;D[3]=X;D[4]=0;D[5]=0;D[6]=-50;D[7]=R;D[8]=0;
```

```

D[9]=600;D[10]=10;D[11]=R;D[12]=0;D[13]=3645;
Lattice(SPIRAL,D,S);SetViewAngle(0,80,-50);DrawFrame(FRAME_NULL,1,0xfffff);
Draw("LINE,0,2,XYZ,0","-150,0,0,-50,0,0");Draw("ARROW,0,2,XYZ,10","50,0,0,150,0,0");
SetPen(2,0xffff0000);Plot("POLYLINE,0,600,XYZ",S[9]);i=9+3*N-6;Draw("ARROW,0,2,XYZ,10",S[i]);
TextHang(S[i],S[i+1],S[i+2]," #if|u|=ic#t");TextHang(150,0,0," #ifx#sd1#t");SetPen(2,0x005fff);
Draw("LINE,1,2,XYZ,8","-50,0,50,-50,0,100");Draw("LINE,1,2,XYZ,8","-40,0,50,-40,0,100");
Draw("ARROW,0,2,XYZ,10","-80,0,100,-50,0,100");Draw("ARROW,0,2,XYZ,10","-10,0,100,-40,0,100");
TextHang(-50,0,110,"1 spiral step");i=9+3*N;S[i]=50;S[i+1]=10;S[i+2]=10;
Draw("ARROW,0,2,XYZ,10","50,0,0,50,80,80");TextHang(50,80,80," #ifx#sd5#t");
Draw("ARROW,0,2,XYZ,10","50,72,0,50,0,72");TextHang(50,0,72," #ifx#sd4#t");
SetPen(3,0x00ffff);Draw("ARROW,0,2,XYZ,15",S[i-3]);TextHang(S[i],S[i+1],S[i+2]," #if|a|=iβ#t");
SetPen(3,0x00ff00);Draw("ARROW,0,2,XYZ,15","50,0,0,120,0,0");TextHang(110,5,5," #ifj#t");
TextHang(-60,0,-80," right hand chirality");;#v07=?>A

```

In analogy with the ball in a circular path, consider a particle in one dimensional motion along the x_1 axis at the speed v , in the Fig.1(b) it moves with the constant speed $|u|=ic$ almost along the x_4 axis and slightly along the x_1 axis, and the constant centripetal acceleration $|\alpha|=i\beta$ in the x_5 axis at the constant radius iR (imaginary number); the coordinate system $(x_1, x_4=ict, x_5=iR)$ establishes a cylinder coordinate system in which this particle moves spirally at the speed v along the x_1 axis. According to usual centripetal acceleration formula $a=v^2/r$, the acceleration in the x_4 - x_5 plane is given by

$$a = \frac{v^2}{r} \Rightarrow i\beta = \frac{|u|^2}{iR} = -\frac{c^2}{iR} = i\frac{c^2}{R} . \quad (7)$$

Therefore, the track of the particle in the cylinder coordinate system $(x_1, x_4=ict, x_5=iR)$ forms a shape, called as **acceleration-roll**. The faster the particle moves along the x_1 axis, the longer the spiral step is.

As like a steel spring with elastic wave, the track in the acceleration-roll in Fig.1(b) can be described by a wave function whose phase changes 2π for one spiral step. **Apparently, this wave is the de Broglie's matter wave for electrons, protons or quarks, etc.**

Proof: The wave function phase changes 2π for one spiral circumference $2\pi(iR)$, then a small displacement of the particle on the spiral track is $|u|d\tau=icd\tau$ in the 4-vector u direction, thus this wave phase along the spiral track is evaluated by

$$phase = \int_0^\tau \frac{2\pi}{2\pi(iR)} icd\tau = \int_0^\tau \frac{c}{R} d\tau . \quad (8)$$

Substituting the radius R into it, the wave function ψ is given by

$$\psi = \exp(-i \cdot phase) = \exp(-i \int_0^\tau \frac{c}{R} d\tau) = \exp(-i \frac{\beta}{c} \int_0^\tau d\tau) . \quad (9)$$

In the theory of relativity, we known that the integral along $d\tau$ needs to transform into realistic line integral, that is

$$\begin{aligned} d\tau &= -c^2 \frac{d\tau}{-c^2} = (u_1^2 + u_2^2 + u_3^2 + u_4^2) \frac{d\tau}{-c^2} \\ &= (u_1 dx_1 + u_2 dx_2 + u_3 dx_3 + u_4 dx_4) \frac{1}{-c^2} \end{aligned} . \quad (10)$$

Therefore, the wave function ψ is evaluated by

$$\begin{aligned}\psi &= \exp(-i \frac{\beta}{c} \int_0^\tau d\tau) \\ &= \exp(i \frac{\beta}{c^3} \int_0^x (u_1 dx_1 + u_2 dx_2 + u_3 dx_3 + u_4 dx_4))\end{aligned}\quad (11)$$

This wave function may have different explanations, depending on the particle under investigation. If the β is replaced by the Planck constant, the wave function of electrons is given by

$$\begin{aligned}\text{assume: } \beta &= \frac{mc^3}{\hbar} \\ \psi &= \exp(\frac{i}{\hbar} \int_0^x (mu_1 dx_1 + mu_2 dx_2 + mu_3 dx_3 + mu_4 dx_4))\end{aligned}\quad (12)$$

where $mu_4 dx_4 = -Edt$, it strongly suggests that the wave function is just the **de Broglie's matter wave** [4,5,6].

In Fig.1(b), the acceleration-roll of particle moves with two distinctions: right-hand chirality and left-hand chirality. The direction of the angular momentum J would be slightly different from the x_1 due to spiral precession. It is easy to calculate the ultimate acceleration β , the radius R and the angular momentum J in the plane x_4 - x_5 for a spiraling electron as

$$\begin{aligned}\beta &= \frac{c^3 m}{\hbar} = 2.327421e+29 \text{ (M/s}^2\text{)} \\ R &= \frac{c^2}{\beta} = 3.861593e-13 \text{ (M)} \\ J &= \pm m |u| iR = \mp \hbar\end{aligned}\quad (13)$$

```
<Clet2020 Script>// Clet is a C compiler[26]
double beta,R,J,m,D[10];char str[200];
int main(){m=ME;beta=SPEEDC*SPEEDC*SPEEDC*m/PLANCKBAR;
R=SPEEDC*SPEEDC/beta;J=PLANCKBAR;Format(str,"beta=%e, #nR=%e, #nJ=%e",beta,R,J);
TextAt(50,50,str);ClipJob(APPEND,str);}#v07=#t
```

Considering another explanation to ψ for planets in the solar system, no Planck constant can be involved. But, in a many-body system with the total mass M , the data-analysis [28] tells us that the ultimate acceleration can be rewritten in terms of **Planck-constant-like constant h** as

$$\begin{aligned}\text{assume: } \beta &= \frac{c^3}{hM} \\ \psi &= \exp(\frac{i}{hM} \int_0^x (u_1 dx_1 + u_2 dx_2 + u_3 dx_3 + u_4 dx_4))\end{aligned}\quad (14)$$

The constant h will be determined by experimental observations. This paper will show that this wave function is applicable to several many-body systems in the solar system, the wave function is called as the **acceleration-roll wave**.

Considering third explanation to ψ for atoms in cells and viruses. Typically, sound speed in water is $v=1450\text{m/s}$, according to $v=f\lambda$, the sound wavelength λ for frequency $1\text{kHz} \text{---} 1\text{Mhz}$ is $1.5\text{m} \text{---} 1.45\text{mm}$. In general, the sound wavelength is larger than cell size, because cell size is about 1 micro . Thus, almost all cells and viruses live in a smaller space which is not sensitive to the sound. The acceleration-roll can provide a kind of wave with a shorter wavelength and lower frequency for

various cells and viruses beyond human-sensitive sound wave [28].

Of course, there is an "ultimate distance" [28] from which the Hubble law can be derived out.

Tip: actually, ones cannot get to see the acceleration-roll of particle in the relativistic space-time $(x_1, x_2, x_3, x_4=ict)$; only get to see it in the cylinder coordinate system $(x_1, x_4=ict, x_5=iR)$.

3. How to determine the ultimate acceleration

In the Bohr's orbit model for planets or satellites, as shown in Fig.2, the circular quantization condition is given in terms of relativistic matter wave in gravity by

$$\left. \begin{array}{l} \frac{\beta}{c^3} \oint_L v_l dl = 2\pi n \\ v_l = \sqrt{\frac{GM}{r}} \end{array} \right\} \Rightarrow \sqrt{r} = \frac{c^3}{\beta\sqrt{GM}} n; \quad n = 0, 1, 2, \dots \quad (15)$$

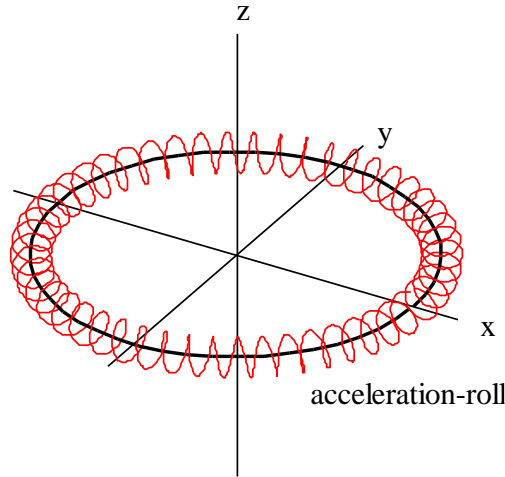


Fig.2 A planet 2D orbit around the sun, an acceleration-roll winding around the planet.

```
<Clet2020 Script>// Clet is a C compiler[26]
int i,j,k; double r,rot,x,y,z,D[20],F[20],S[200];
int main(){SetViewAngle("temp0,theta60,phi-30");
DrawFrame(FRAME_LINE,1,0xff00);r=80;Spiral(); TextHang(r,-r,0,"acceleration-roll");
r=110;TextHang(r,0,0,"x");TextHang(0,r,0,"y");TextHang(0,0,r,"z");}
Spiral(){r=80;j=10;rot=j/r;k=2*PI/rot+1;
for(i=0;i<k;i+=1){D[0]=x;D[1]=y;D[2]=z;D[6]=x;D[7]=y;D[8]=r;
x=r*cos(rot*i);y=r*sin(rot*i);z=0;if(i==0) continue;
SetPen(2,0x00);F[0]=D[0];F[1]=D[1];F[2]=x;F[3]=y;Draw("LINE,0.2,XY",F);SetPen(1,0xff0000);
D[3]=x;D[4]=y;D[5]=z; D[9]=40;D[10]=10;D[11]=8;D[12]=0;D[13]=360;
Lattice(SPIRAL,D,S);Plot("POLYLINE,0.40,XYZ",S[9]);}
}#v07=?>A
```

The solar system, Jupiter's satellites, Saturn's satellites, Uranus' satellites, Neptune's satellites as five different many-body systems are investigated with the Bohr's orbit model. After fitting observational data as shown in Fig.3, their ultimate accelerations are obtained in Table 1. The predicted quantization-blue-lines in Fig.3(a), Fig.3(b), Fig.3(c), Fig.3(d) and Fig.3(e) agree well with experimental observations for those *inner constituent planets or satellites*.

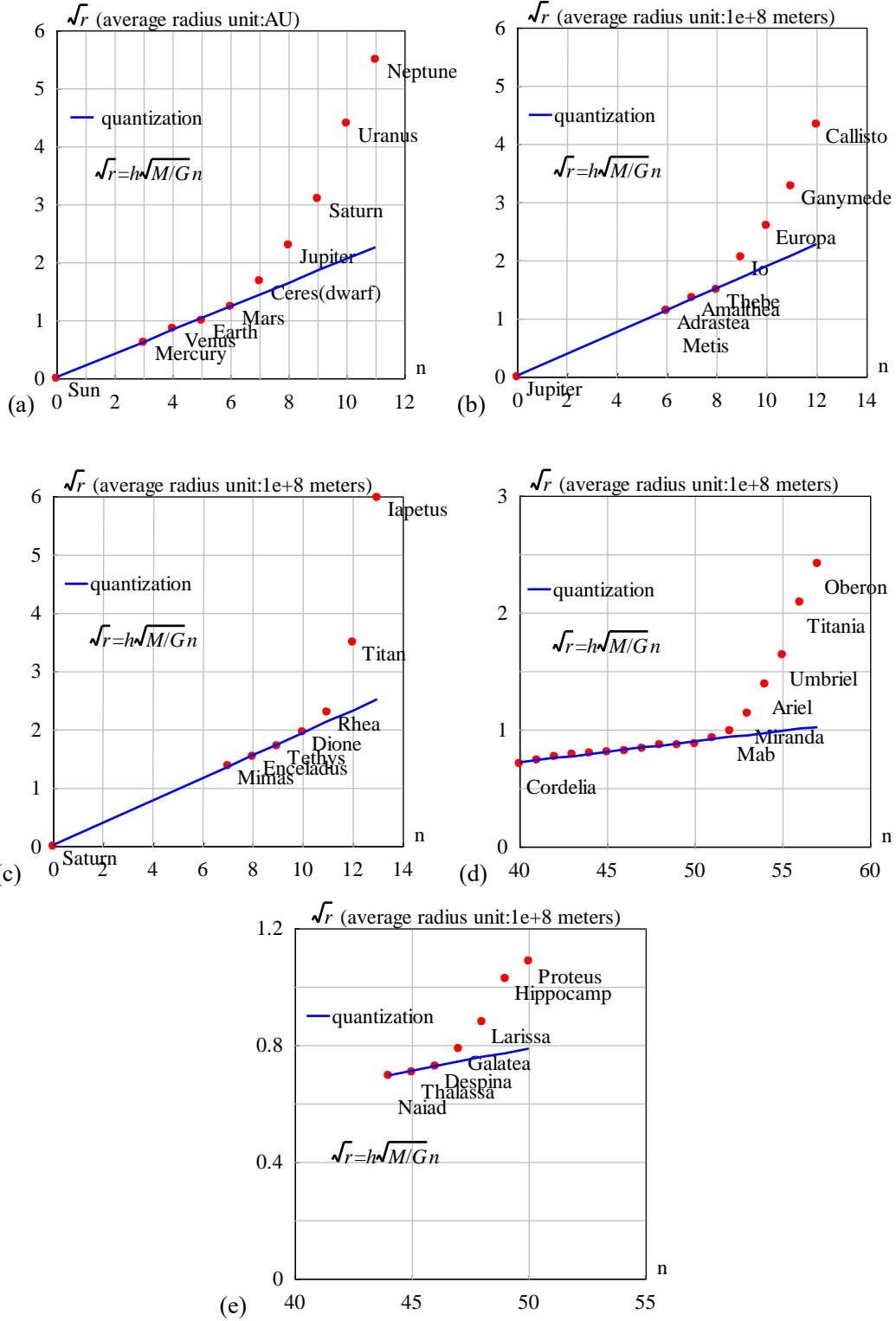


Fig.3 The orbital radii are quantized for inner constituents. (a) the solar system with $h=4.574635e-16$ ($m^2s^{-1}kg^{-1}$). The relative error is less than 3.9%. (b) the Jupiter system with $h=3.531903e-16$ ($m^2s^{-1}kg^{-1}$). Metis and Adrastea are assigned the same quantum number for their almost same radius. The relative error is less than 1.9%. (c) the Saturn system with $h=6.610920e-16$ ($m^2s^{-1}kg^{-1}$). The relative error is less than 1.1%. (d) the Uranus system with $h=1.567124e-16$ ($m^2s^{-1}kg^{-1}$). $n=0$ is assigned to the Uranus. The relative error is less than 2.5%. (e) the Neptune system with $h=1.277170e-16$ ($m^2s^{-1}kg^{-1}$). $n=0$ is assigned to the Neptune. The relative error is less than 0.17%.

Table 1 Planck-constant-like constant h , N is constituent particle number with smaller inclination.

system	N	M/M_{earth}	β (m/s ²)	h (m ² s ⁻¹ kg ⁻¹)	Prediction
Solar planets	9	333000	2.961520e+10	4.574635e-16	Fig.3(a)
Jupiter' satellites	7	318	4.016793e+13	3.531903e-16	Fig.3(b)
Saturn's satellites	7	95	7.183397e+13	6.610920e-16	Fig.3(c)
Uranus' satellites	18	14.5	1.985382e+15	1.567124e-16	Fig.3(d)
Neptune 's satellites	7	17	2.077868e+15	1.277170e-16	Fig.3(e)

Besides every β , our interest shifts to the constant h in Table 1, which is defined as

$$h = \frac{c^3}{M\beta} \Rightarrow \sqrt{r} = h\sqrt{\frac{M}{G}}n \quad (16)$$

In a many-body system with the total mass M , a constituent particle has the mass m and moves at the speed v , it is easy to find that the wavelength of de Broglie's matter wave should be modified for planets and satellites as

$$\lambda_{de_Broglie} = \frac{2\pi\hbar}{mv} \Rightarrow \text{modify} \Rightarrow \lambda = \frac{2\pi hM}{v} \quad (17)$$

where h is a **Planck-constant-like constant**. Usually the total mass M is approximately equal to the central-star's mass. It is found that this modified matter wave works for quantizing orbits correctly in Fig.3 [28,29]. The key point is that the various systems have almost same Planck-constant-like constant h in Table 1 with a mean value of $3.51\text{e-}16$ m²s⁻¹kg⁻¹, at least have the same magnitude! The acceleration-roll wave is a generalized matter wave as a planetary scale wave.

In Fig.3(a), the blue straight line expresses the linear regression relation among the Sun, Mercury, Venus, Earth and Mars, their quantization parameters are $hM=9.098031\text{e+}14$ (m²/s). The ultimate acceleration is fitted out to be $\beta=2.961520\text{e+}10$ (m/s²). Where, $n=3,4,5,\dots$ were assigned to solar planets, the sun was assigned a quantum number $n=0$ because the sun is in the **central state**.

4. Optical model of the central state

The acceleration-roll wave as the relativistic matter wave generalized in gravity is given by

$$\psi = \exp\left(\frac{i}{hM} \int_0^x v_l dl\right); \quad \lambda = \frac{2\pi hM}{v_l} \quad (18)$$

In a central state $n=0$, if the coherent length of the acceleration-roll wave is long enough, its head may overlap with its tail when the particle moves in a closed orbit in the space time, as shown in Fig.4, the interference of the acceleration-roll wave between its head and tail will occur in the overlapping zone. The overlapped wave is given by

$$\psi(r) = 1 + e^{i\delta} + e^{i2\delta} + \dots + e^{i(N-1)\delta} = \frac{1 - \exp(iN\delta)}{1 - \exp(i\delta)} \quad (19)$$

$$\delta(r) = \frac{1}{hM} \oint_L (v_l) dl = \frac{2\pi\omega r^2}{hM} = \frac{2\pi\beta\omega r^2}{c^3}$$

where N is the overlapping number which is determined by the coherent length of the acceleration-roll wave, δ is the phase difference after one orbital motion, ω is the angular speed of the sun rotation. The above equation is a multi-slit interference formula in optics, for a larger N it is called as the Fabry-Perot interference formula.

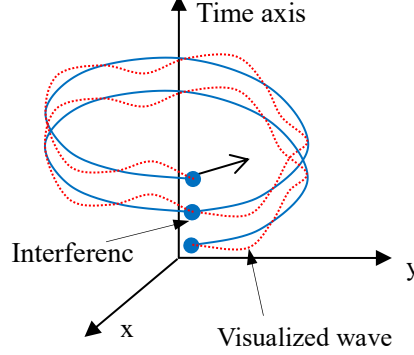


Fig.4 The head of the acceleration-roll wave may overlap with its tail.

The acceleration-roll wave function ψ needs a further explanation. In quantum mechanics, $|\psi|^2$ equals to the probability of finding an electron due to Max Burn's explanation; in astrophysics, $|\psi|^2$ equals to the probability of finding a nucleon (proton or neutron) *averagely in astronomic scale*, because all mass is mainly made of nucleons, we have

$$|\psi|^2 \propto \text{nucleon_density} \quad (20)$$

It follows from the multi-slit interference formula that the interference intensity at maxima is proportional to N^2 , that is

$$N^2 = \frac{|\psi(0)_{\text{multi-wavelet}}|^2}{|\psi(0)_{\text{one-wavelet}}|^2} \quad (21)$$

What matter plays the role of “one-wavelet” in the solar core or Earth core? We choose vapor above the sea on the earth surface as the “reference matter: one-wavelet”. Thus, the overlapping number N is estimated by

$$N^2 = \frac{|\psi(0)_{\text{multi-wavelet}}|^2}{|\psi(0)_{\text{one-wavelet}}|^2} \approx \frac{\text{core_nucleon_density}_{r=0}}{\text{vapor_above_sea_density}} \quad (22)$$

Although today there is not vapor on the solar surface, the solar core has a maximum density of $1.5e+5 \text{ kg/m}^3$ [31], comparing to the vapor density 1.29 kg/m^3 on the earth, the solar overlapping number N is estimated as $N=341$. The Earth core density is $5.53e+3 \text{ kg/m}^3$, the Earth's overlapping number N is estimated as $N=65$.

For the Sun, Earth and Mars, their central densities and their reference matter density are given in the Table 2. Thus, their overlapping numbers are estimated also in this table.

Table 2 Estimating the overlapping number N by comparing solid core to reference matter, regarding protons and neutrons as basis particles.

object	Solid core, density (kg/m ³)	Reference matter, density (kg/m ³)	Overlapping number N	β (m/s ²)
Sun	1.5e+5 (max.)	1.29 (vapor above the sea)	341	2.961520e+10

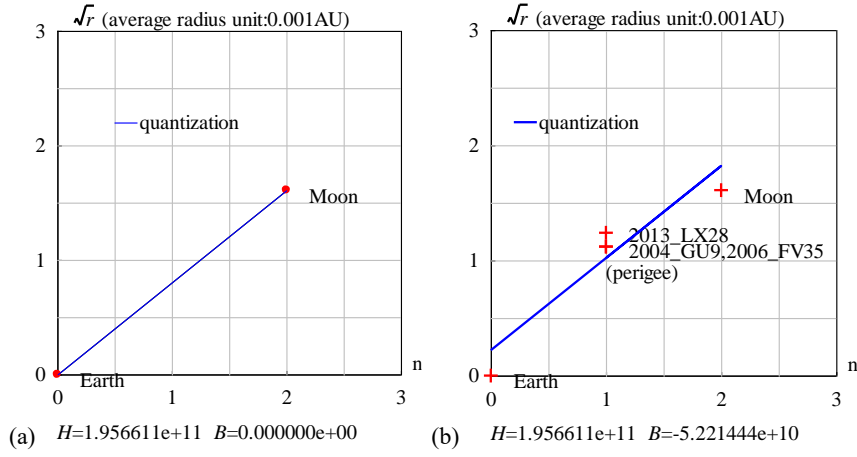


Fig.6 orbital quantization for moon and quasi-satellites to the Earth, $H=hM$.

```

<Clet2020 Script>// Clet is a C compiler[26]
char str[200];int i,j,k,N,nP[10]; double x,y,z,M,r_unit,a,b,B,H,r_ave[20],dP[10],D[1000];
double orbit[10]={0,2.57,0,}; double e[10]={0, 0.0549,0,0,0,0,0,0,0,0,};
int qn[10]={0,2,3,4,5,6,7,8,9,10,};
char Stars[100]={"Earth;Moon;"};
int main(){ N=2; M=5.97237E24; r_unit=1.495978707e8;
for(i=0;i<N;i+=1) {x=orbit[i];y=e[i]; z=x*(1+sqrt(1-y*y))/2;r_ave[i]=z;//average_radius
D[i+i]=qn[i];D[i+i+1]=sqrt(z); }
DataJob("REGRESSION,2",D,dP);b=dP[0];a=dP[1];
SetAxis(X_AXIS,0,0,3,"n;0;1;2;3;");
SetAxis(Y_AXIS,0,0,3," #if#r#t#t (average radius unit:0.001AU);0;1;2;3;");
DrawFrame(0x0166,1,0xaffaf); Polyline(N,D);
SetPen(2,0xff0000); Plot("OVALFILL,0.2,XY,3,3, ",D);
for(i=0;i<N;i+=1) {nP[0]=TAKE;nP[1]=i;TextJob(nP,Stars,str);x=qn[i]+0.2;y=sqrt(orbit[i])-0.05;TextHang(x,y,0,str);}
x=GRAVITYC*M*r_unit; z=sqrt(x); H=z*a; B=-z*b;
TextAt(100,450,"#if#t=#e #ifB#t=#e",H,B);
for(i=0;i<N;i+=1) {y=b+a*qn[i];D[i+i]=qn[i];D[i+i+1]=y;}
SetPen(1,0x0000ff);Polyline(N,D,0.5,2.2,"quantization");//check
}}#v07=?>A

```

Now let us talk about the central state of the earth, the earth's rotation angular speed is known as $\omega=2\pi/(24*3600)$, unit s^{-1} . Its mass $5.97237e+24$ (kg), radius $6.371e+6$ (m), core density 5530 (kg/m^3), the ultimate acceleration $\beta=1.377075e+14$ (m/s^2), the constant $hM=1.956611e+11$ (m^2/s).

We have estimated that the wave overlapping number in the central state of the earth is $N=65$, the matter distribution $|\psi|^2$ in radius direction is calculated out as shown in Fig.7(a), where the self-rotation near its equator has the period of 24 hours:

$$\delta(r) = \frac{1}{hM} \oint_L (v_i) dl = \frac{2\pi r}{hM} \omega r \quad (23)$$

There is a central maximum of matter distribution at the earth heart, which gradually decreases to zero near the earth surface, then rises the secondary peaks and attenuates down off. The radius of the earth is calculated out to be $r=6.4328e+6$ (m) with a relative error 0.97% using the interference of its acceleration-roll wave. Space debris over the atmosphere has a complicated evolution [7,8], has itself speed

$$v_i = \sqrt{\frac{GM}{r}}; \quad \delta(r) = \frac{1}{hM} \oint_L (v_i) dl = \frac{\beta}{c^3} \oint_L (v_i) dl = \frac{2\pi\beta}{c^3} \sqrt{GMr} \quad (24)$$

The secondary peaks over the atmosphere up to 2000km altitude is calculated out in Fig.7(b) which agrees well with the space debris observations [16]; the peak near 890 km altitude is due principally to the January 2007 intentional destruction of the Fengyun-1C weather spacecraft while the peak centered at approximately 770 km altitude was created by the February 2009 accidental collision of

Iridium 33 (active) and Cosmos 2251 (derelict) communication spacecraft [16,18]. The observations based on the incoherent scattering radar EISCAT ESR located at 78°N in Jul. 2006 and in Oct. 2015 [21,22,23] are respectively shown in Fig.7(c) and (d). This prediction to secondary peaks also agrees well with other space debris observations [24,25].

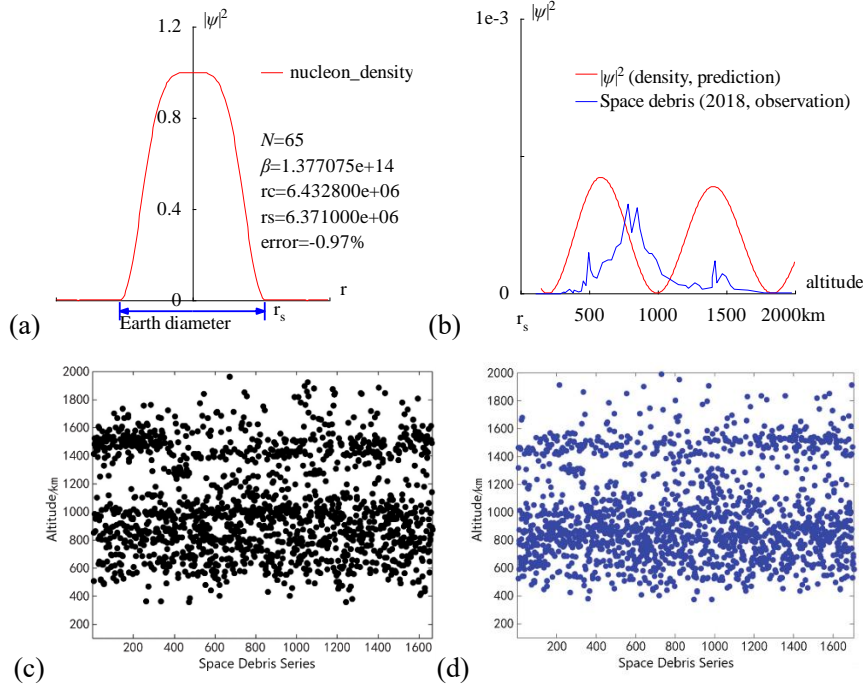


Fig.7 (a) The radius of the Earth is calculated out $r=6.4328e+6$ (m) with a relative error 0.97% by the interference of its acceleration-roll wave; (b) The prediction of the space debris distribution up to 2000km altitude; (c) The space debris distribution in Jul. 2006, Joint observation based on the incoherent scattering radar EISCAT ESR located at 78°N [21]; (d) The space debris distribution in Oct. 2015, Joint observation based on the incoherent scattering radar EISCAT ESR located at 78°N [21].

<Clet2020 Script>// Clet is a C compiler[26]

```
int i,j,k,m,n,N,nP[10];
double H,B,M,v_r,r,AU,r_unit,x,y,z,delta,D[10],S[1000];
double rs,rc,rot,a,b,atm_height,beta; char str[100];
main(){k=80;rs=6.371e6;rc=0;atm_height=1.5e5;n=0; N=65;
beta=1.377075e+14;H=SPEEDC*SPEEDC*SPEEDC/beta;
M=5.97237e24;AU=1.496E11;r_unit=1e-6*AU;
rot=2*PI/(24*60*60);//angular speed of the Earth
for(i=-k;i<k;i+=1){r=abs(i)*r_unit;
if(r<rs+atm_height)v_r=rot*r; else v_r=sqrt(GRAVITYC*M/r);//around the Earth
delta=2*PI*v_r/H; y=SumJob("SLIT_ADD,@N,@delta",D); y=y/(N*N);
if(y>1)y=1; S[n]=i;S[n+1]=y; if(i>0 && rc=0 && y<0.001)rc=r; n+=2;}
SetAxis(X_AXIS,-k,0,k,"r"; ; );SetAxis(Y_AXIS,0,0,1.2,"#i f|ψ|#su2#t;0;0.4;0.8;1.2;");
DrawFrame(FRAME_SCALE,1,0xaffaf); x=50;z=100*(rs-rc)/rs;
SetPen(1,0xff0000);Polyline(k+k,S,k/2,1,"nucleon density");
r=rs/r_unit;y=-0.05;D[0]=r;D[1]=y;D[2]=r;D[3]=y;
SetPen(2,0x0000ff); Draw("ARROW,3,2,XY,10,100,10,10,",D);
Format(str,"#i f|ψ|#su2#t;0;0.4;0.8;1.2;");
TextHang(k/2,0.7,0,str);TextHang(r+5,y/2,0,"r#sds#t");TextHang(-r,y+y,0,"Earth diameter");
}#v07=?>A
```

<Clet2020 Script>//Clet is a C compiler[26]

```
int i,j,k,m,n,N,nP[10]; double H,B,M,v_r,r,AU,r_unit,x,y,z,delta,D[10],S[10000];
double rs,rc,rot,a,b,atm_height,p,T,R1,R2,R3; char str[100];
int
Debris[96]={110,0,237,0,287,0,317,2,320,1,357,5,380,1,387,4,420,2,440,3,454,14,474,9,497,45,507,26,527,19,557,17,597,34,63
4,37,664,37,697,51,727,55,781,98,808,67,851,94,871,71,901,50,938,44,958,44,991,37,1028,21,1078,17,1148,10,1202,9,1225,6,
1268,12,1302,9,1325,5,1395,7,1395,18,1415,36,1429,12,1469,22,1499,19,1529,9,1559,5,1656,4,1779,1,1976,1,};
main(){k=80;rs=6.371e6;rc=0;atm_height=1.5e5;n=0; N=65;
H=1.956611e11;M=5.97237e24;AU=1.496E11;r_unit=1e4;
rot=2*PI/(24*60*60);//angular speed of the Earth
b=PI/(2*PI*rot*rs/H); R1=rs/r_unit;R2=(rs+atm_height)/r_unit;R3=(rs+2e6)/r_unit;
for(i=R2;i<R3;i+=1){r=abs(i)*r_unit; delta=2*PI*sqrt(GRAVITYC*M/r)/H;
y=SumJob("SLIT_ADD,@N,@delta",D); y=1e3*y/(N*N);// visualization scale:1000
if(y>1)y=1; S[n]=i;S[n+1]=y;n+=2;}
```

```

SetAxis(X_AXIS,R1,R1,R3,"altitude; r#sds#t;500;1000;1500;2000km ;");
SetAxis(Y_AXIS,0,0,1,"#if#w/#su2#t;0; ;1e-3;");DrawFrame(FRAME_SCALE,1,0xaffaf); x=R1+(R3-R1)/5;
SetPen(1,0xff0000);Polyline(n/2,S,x,0.8,"#if#w/#su2#t (density, prediction)");
for(i=0;i<48;i+=1) {S[i+1]=R1+(R3-R1)*Debris[i+1]/2000; S[i+1+1]=Debris[i+1+1]/300;}
SetPen(1,0x0000ff);Polyline(48,S,x,0.7,"Space debris (2018, observation) ");
}#v07=?>A

```

6. Mars and Jovian planets

The Mars and its satellites are quantized very well by its ultimate acceleration β as shown in Fig.8(a). Now let us talk about the Mars in the central state with quantum number $n=0$, its ultimate acceleration is $\beta=2.581555e+15(m/s^2)$ in the Mars system. We have estimated the Mars overlapping number $N=55$ in Table 2, the matter distribution $|\psi|^2$ around the Mars can be calculated out in radius direction as shown in Fig.8(b), where the self-rotation at equator has the period of 24 hours.

The radius of the Mars is calculated out as $r=1.6e+6$ (m) with a relative error 52.79%, no further attempt was made to improve the calculation, because of limited knowledge about the Mars history. But one thing is certain, the Mars has frequently bombarded with smaller objects, in fact, consequently with the inclination of 25.2 degrees, so that its self-rotation is unstable or incorrect for its formation in a sense. At very beginning, the Mars self-rotation should have a period of 100 hours. Thanks to the Mars for safeguarding the Earth.

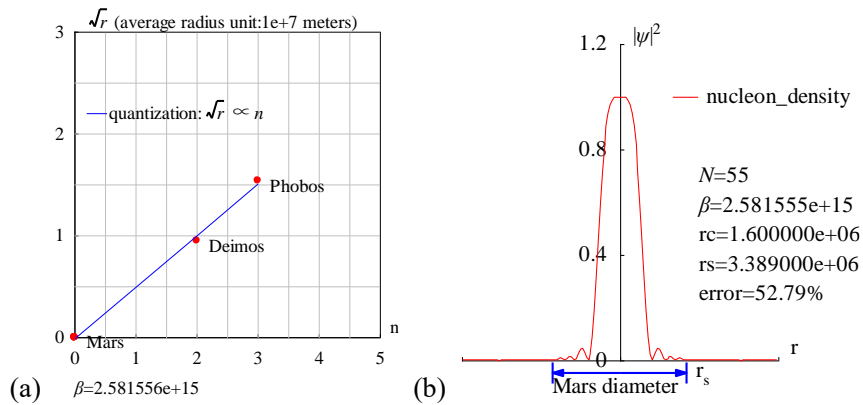


Fig.8 (a)Quantization of Mars and its satellites. (b)The matter distribution $|\psi|^2$ around the Mars has been calculated in radius direction.

```

<Clet2020 Script>//Clet is a C compiler[26]
int i,j,k,m,n,N,nP[10];
double H,B,M,v_r,r,AU,r_unit,x,y,z,delta,D[10],S[1000],F[1000];
double rs,rc,rot,a,b,atm_height,beta; char str[100];
main(){k=80;rs=3.389e6;rc=0;atm_height=10e3;n=0; N=55;
beta=2.581555e+15; H=SPEEDC*SPEEDC*SPEEDC/beta;
M=0.107*5.97237e24; AU=1.496E11;r_unit=1e5;
rot=2*PI/(24*60*60);//angular speed
for(i=-k;i<k;i+=1) {r=abs(i)*r_unit;
if(r<rs+atm_height) v_r=rot*r; else v_r=sqrt(GRAVITYC*M/r);//around the star
delta=2*PI*v_r/H;y=SumJob("SLIT_ADD,@N,@delta",D); y=y/(N*N);
if(y>1) y=1; S[n]=i;S[n+1]=y; if(i>0 && rc==0 && y<0.001) rc=r; n+=2;}
SetAxis(X_AXIS,-k,0,k,"r; ;");SetAxis(Y_AXIS,0,0,1.2,"#if#w/#su2#t;0;0.4;0.8;1.2;");
DrawFrame(FRAME_SCALE,1,0xaffaf); x=50;z=100*(rs-rc)/rs;
SetPen(1,0xff0000);Polyline(k+k,S,k/3,1," nucleon_density");
r=rs/r_unit;y=-0.05;D[0]=-r;D[1]=y;D[2]=r;D[3]=y;
SetPen(2,0x0000ff); Draw("ARROW,3,2,XY,10,100,10,10,"D);
Format(str,"#ifN#t=%d#n#i#t=%e#nrc=%e#nrs=%e#nerror=%.2f%",N,beta,rc,rs,z);
TextHang(k/2,0.7,0,str);TextHang(r+5,y/2,0,"#sds#t"); TextHang(-r,y+0,"Mars diameter");
}#v07=?>A

```

In order to extend the quantization rule to the Jovian planets (Jupiter, Saturn, Uranus and Neptune), it is necessary to further study the magnet-like components of gravity [28], the issue beyond the scope of this paper.

7. New aspect: coherent width and Sunspot cycle

It is common to mention **coherent length** of a wave, but one rarely talks about **coherent width** of a wave in quantum mechanics, simply because the latter is not a matter for electrons, nucleon or photos, but it is a matter in astrophysics. Analyzing observational data tells us that the coherent width of an acceleration-roll wave can extend to a 1000km or even more in planetary scale, as illustrated in Fig.9(a), the overlapping can even happen in width-direction bringing with a new aspect for wave interference.

In the solar convective zone, adjacent convective arrays form a top-layer flow, a middle-layer gas and a ground-layer reverse flow, (like the concept of **molecular current** in electromagnetism). Considering one convective ring at the equator as shown in Fig.9(b), there is an apparent velocity difference between the top-layer flow and the middle-layer gas, where their acceleration-roll waves are denoted respectively by

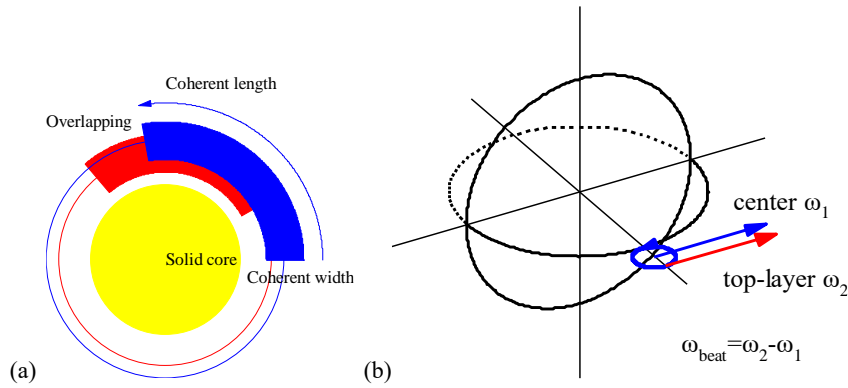


Fig.9 (a) Illustration of overlapping in coherent width direction. (b)One convective ring at the equator, the speed difference causes a beat frequency.

<Clet2020 Script>//Clet is a C compiler[26]

```
int i, j, k, R, D[500];
main(){DrawFrame(FRAME_NULL,1,0xffff00);
R=60; SetPen(1,0xffff00);
D[0]=-R; D[1]=-R; D[2]=R; D[3]=R; Draw("ELLIPSE,1,2,XY,0",D);
R=85; k=15; SetPen(1,0xff0000);
D[0]=-R; D[1]=-R; D[2]=R; D[3]=R; Draw("ELLIPSE,0,2,XY,0",D);
D[0]=0; D[1]=0; D[2]=R-k; D[3]=0; D[4]=R+k;D[5]=0;
Draw("SECTOR,1,3,XY,15,30,130,0",D);
R=95; k=15; SetPen(1,0x00ff);
D[0]=-R; D[1]=-R; D[2]=R; D[3]=R; Draw("ELLIPSE,0,2,XY,0",D);
D[0]=0; D[1]=0; D[2]=R-k; D[3]=0; D[4]=R+k;D[5]=0;
Draw("SECTOR,1,3,XY,15,0,100,0",D);D[4]=R+k+k;
Draw("SECTOR,3,3,XY,15,0,100,0",D);
TextHang(0,0,0,"Solid core");TextHang(R-k-k,-k,0,"Coherent width");
TextHang(0,R+k+k+k,0,"Coherent length");TextHang(-R,R+k,0,"Overlapping");
}#v07=?>A
```

<Clet2020 Script>//Clet is a C compiler[26]

```
double beta,H,M,N,dP[20],D[2000],r,rs,rot,x,y,v1,v2,K1,K2,T1,T2,T,Lamda,V;
int main(){beta=2.961520e10; H=SPEEDC*SPEEDC*SPEEDC/beta;
M=1.9891E30; rs=6.95e8;rot=2*PI/(25.05*24*3600);v1=rot*rs;K1=v1*v1/2;//T1=2*PI*H/K1;
v2=0.7346*sqrt(BOLTZMANN*5700/MP)+0.2485*sqrt(BOLTZMANN*5700/(MP+MP));
K2=v2*v2/2;T2=2*PI*H/(K2-K1);T=T2/24*3600*365.2422;
Lamda=2*PI*H/(v2-v1);V=Lamda/T2;
SetViewAngle("temp0,theta60,phi-60");
DrawFrame(FRAME_LINE,1,0xffff00);Overlook("2,1,60", D);
TextAt(10,10,"v1=%d, v2=%d, T=%f y, λ=%e, V=%d",v1,v2,T, Lamda,V);
TextJob("14","70,0,0,70,0,20,80,0,0,200,10,10,0",dP);Lattice(OVAL,dP,D);
SetPen(3,0x4f4fff);Plot("POLYLINE,4,200,XYZ,10",D[9]);
SetPen(2,0xffff00);Draw("ARROW,0,2,XYZ,15","80,0,0,80,60,0");
TextHang(100,20,0,"top-layer ω#sd2#t"); SetPen(2,0x0000ff);
Draw("ARROW,0,2,XYZ,15","70,0,0,70,60,0");
TextHang(40,60,0,"center ω#sd1#t");TextHang(140,-30,0," ω#sdbeat#t=ω#sd2#t-ω#sd1#t");
}#v07=?>A
```

$$\begin{aligned}\psi &= \psi_{middle} + C\psi_{top} \\ \psi_{middle} &= \exp\left[\frac{i\beta}{c^3} \int_L (v_1 dl + \frac{-c^2}{\sqrt{1-v_1^2/c^2}} dt)\right] \\ \psi_{top} &= \exp\left[\frac{i\beta}{c^3} \int_L (v_2 dl + \frac{-c^2}{\sqrt{1-v_2^2/c^2}} dt)\right]\end{aligned}\quad (25)$$

Where, we simply suppose the couple coefficient to be $C=1$, their overlapping wave interference in coherent width direction leads to a beat phenomenon

$$\begin{aligned}|\psi|^2 &= |\psi_{middle} + \psi_{top}|^2 = 2 + 2 \cos\left[\frac{2\pi}{\lambda_{beat}} \int_L dl - \frac{2\pi}{T_{beat}} t\right] \\ \frac{2\pi}{T_{beat}} &= \frac{\beta}{c^3} \left(\frac{c^2}{\sqrt{1-v_2^2/c^2}} - \frac{c^2}{\sqrt{1-v_1^2/c^2}} \right) \approx \frac{\beta}{c^3} \left(\frac{v_2^2}{2} - \frac{v_1^2}{2} \right) \\ \frac{2\pi}{\lambda_{beat}} &= \frac{\beta}{c^3} (v_2 - v_1); \quad V = \frac{\lambda_{beat}}{T_{beat}} = \frac{1}{2} (v_2 + v_1)\end{aligned}\quad (26)$$

Their speeds are calculated by

$$\begin{aligned}v_1 &= \omega r_{middle} = 2017 \text{ (m/s)} \quad (\text{sun rotation}); \\ v_2 &\approx 6200 \text{ (m/s)} \quad (\approx \text{observed in Evershed flow})\end{aligned}\quad (27)$$

There are three ways to estimate the top-layer flow speed v_2 . (1) regarding the Evershed flow as the eruption of the top-layer flow, about 6km/s speed was reported [31]. (2) regarding the prominences as the eruption of the top-layer flow; the prominence turbulent speeds are reported [31] in the range 2-10km/s. (3) Alternatively, since the thermal equilibrium gas in a convective zone supplies the flow speed v_2 , where the temperature $T=5700^\circ\text{K}$, the flow consists of 73.46% hydrogen atoms and 24.85% helium atoms; these atoms are approximately regarded as in 1D circular flow: $mv^2/2=kT/2$. Thus, the top-layer speed v_2 can be estimated out by

$$\begin{aligned}v_2 &\approx 0.7346 \sqrt{\frac{kT}{m_{hydrogen}}} + 0.2485 \sqrt{\frac{kT}{m_{helium}}} \\ &= 6244 \text{ (m/s)}\end{aligned}\quad (28)$$

Their beat period T_{beat} is calculated out to be a very remarkable value 10.38 (years), in agreement with the sunspot cycle value (say, mean 11years).

$$T_{beat} \approx \frac{4\pi c^3}{\beta(v_2^2 - v_1^2)} = 10.38 \text{ (years)} \quad (29)$$

The relative error to the mean 11 years is 5.6% for the beat period calculation using the acceleration-roll waves. This beat turns out to be a [nucleon density wave](#) that undergoes to drive the sunspot cycle evolution. Comparing to the beat wavelength λ_{beat} , in order of magnitude, only the beat period is easy to be observed. This nucleon density wave is understood as a [new type nuclear reaction](#) in astronomic scale.

In the above calculation, although this seems to be a rough model, there is an obvious correlation between solar radius, solar rotation, solar density, ultimate acceleration and Planck-

constant-like constant h .

8. The El Niño Oscillation in the Earth ocean

Now we discuss the beat phenomenon between the oceans and the atmospheric circulation near the equator via width-direction interference to their acceleration-roll waves.

The trade winds or easterlies are the permanent east-to-west prevailing winds that flow in the Earth's equatorial region. The trade winds blow mainly from the northeast in the Northern Hemisphere and from the southeast in the Southern Hemisphere, strengthening during the winter and when the Arctic oscillation is in its warm phase. Trade winds have been used by captains of sailing ships to cross the world's oceans for centuries. The driving force of atmospheric circulation is the uneven distribution of solar heating across the earth, which is greatest near the equator and least at the poles. This air rises to the tropopause, about 10–15 kilometers above sea level, where the air is no longer buoyant [33].

As a simplest model, regarding the ocean as a static massive matter with the earth self-rotation speed $v_1 = \omega r = 463 \text{ m/s}$ at the equator, approximately estimating the mean speed of the atmospheric circulation at the equator as $v_2 = v_1 - 10 \text{ m/s}$, (magnitude order estimation), then they give out their beat period as

$$T_{beat} \approx \frac{4\pi c^3}{\beta(v_2^2 - v_1^2)} = 8.23 \text{ (years)} . \quad (30)$$

```
<Clet2020 Script>//Clet is a C compiler[26]
double beta,H,M,N,dP[20],D[2000],r,rc,rs,rot,x,y,z,v1,v2,K1,K2,T1,T2,T,Lamda,V; char str[100];
int main(){beta=1.377075e+14; H=SPEEDC*SPEEDC*SPEEDC/beta;
M=5.97237e24; rs=6.371e6; rot=2*PI/(24*3600);v1=rot*rs;K1=v1*v1/2;//T1=2*PI*H/K1;
v2=v1+10;//sqrt(M*GRAVITYC/rs);//1023;
K2=v2*v2/2;T2=2*PI*H/(K2-K1);T=T2/24*3600*365.2422;
Lamda=2*PI*H/(v2-v1);V=Lamda/T2;
TextAt(10,10,"v1=%d, v2=%d, T=%f y, λ=%e, V=%d",v1,v2,T, Lamda,V);
}#v07=?>A
```

This beat turns out to be a [nucleon density wave](#) that undergoes to drive the cycle evolution. This period 8.23 years of the nucleon density wave on the earth surface is also a remarkable cycle. It is easy to find that the ocean variation near the equator seems having an apparent respond to this cycle. El Niño–Southern Oscillation (ENSO) is an irregular periodic variation (4 years—10 years) in winds and sea surface temperatures over the tropical eastern Pacific Ocean, affecting the climate of much of the tropics and subtropics. The warming phase of the sea temperature is known as El Niño and the cooling phase as La Niña. The Southern Oscillation is the accompanying atmospheric component, coupled with the sea temperature change: El Niño is accompanied by high air surface pressure in the tropical western Pacific and La Niña with low air surface pressure there. The two periods last several months each and typically occur every few years with varying intensity per period [33].

9. Conclusions

In general, some quantum gravity proposals [1,2] are extremely hard to test in practice, as

quantum gravitational effects are appreciable only at the Planck scale [3]. But ultimate acceleration gives another scheme to enhance the quantum gravity effects. In analogy with the ultimate speed c , there is an ultimate acceleration β , nobody's acceleration can exceed this limit β , in the solar system, $\beta=2.961520e+10(m/s^2)$. Because this ultimate acceleration is a large number, any effect connecting to β will become easy to test, including quantum gravity tests. In this paper, an approach is put forward to connect the ultimate acceleration with quantum theory, as an application, this relativistic model gives out the sunspot cycle to be 10.38 years due to the ultimate acceleration. The same approach is applied to the Earth El Niño oscillation, calculating out the El Niño irregular period to be 8.23 years.

References

- [1]C. Marletto, and V. Vedral, Gravitationally Induced Entanglement between Two Massive Particles is Sufficient Evidence of Quantum Effects in Gravity, *Phys. Rev. Lett.*, 119, 240402 (2017)
- [2]T. Guerreiro, Quantum effects in gravity waves, *Classical and Quantum Gravity*, 37 (2020) 155001 (13pp).
- [3]S. Carlip, D. Chiou, W. Ni, R. Woodard, Quantum Gravity: A Brief History of Ideas and Some Prospects, *International Journal of Modern Physics D*, V,24,14,2015,1530028. DOI:10.1142/S0218271815300281.
- [4]de Broglie, L., *CRAS*,175(1922):811-813, translated in 2012 by H. C. Shen in *Selected works of de Broglie*.
- [5]de Broglie, *Waves and quanta*, *Nature*, 112, 2815(1923): 540.
- [6]de Broglie, *Recherches sur la théorie des Quanta*, translated in 2004 by A. F. Kracklauer as *De Broglie, Louis, On the Theory of Quanta*. 1925.
- [7]NASA, <https://solarscience.msfc.nasa.gov/interior.shtml>.
- [8]NASA, <https://nssdc.gsfc.nasa.gov/planetary/factsheet/marsfact.html>.
- [9]B. Ryden *Introduction to Cosmology*, Cambridge University Press, 2019, 2nd edition.
- [10]D. Valencia, D. D. Sasselov, R. J. O'Connell, Radius and structure models of the first super-earth planet, *The Astrophysical Journal*, 656:545-551, 2007, February 10.
- [11]D. Valencia, D. D. Sasselov, R. J. O'Connell, Detailed models of super-earths: how well can we infer bulk properties? *The Astrophysical Journal*, 665:1413–1420, 2007 August 20.
- [12]T. Guillot, A. P. Showman, Evolution of "51Pegabus-like" planets, *Astronomy & Astrophysics*,2002, 385,156-165, DOI: 10.1051/0004-6361:20011624
- [13]T. Guillot, A. P. Showman, Atmospheric circulation and tides of "51Pegabus-like" planets, *Astronomy & Astrophysics*,2002, 385,166-180, DOI: 10.1051/0004-6361:20020101
- [14]L.N. Fletcher, Y.Kaspi, T. Guillot, A.P. Showman, How Well Do We Understand the Belt/Zone Circulation of Giant Planet Atmospheres? *Space Sci Rev*, 2020,216:30. <https://doi.org/10.1007/s11214-019-0631-9>
- [15]Y. Kaspi, E. Galanti, A.P. Showman, D. J. Stevenson, T. Guillot, L. Iess, S.J. Bolton, Comparison of the Deep Atmospheric Dynamics of Jupiter and Saturn in Light of the Juno and Cassini Gravity Measurements, *Space Sci Rev*, 2020, 216:84. <https://doi.org/10.1007/s11214-020-00705-7>
- [16]Orbital Debris Program Office, *HISTORY OF ON-ORBIT SATELLITE FRAGMENTATIONS*, National Aeronautics and Space Administration, 2018, 15 th Edition.
- [17]M. Mulrooney, The NASA Liquid Mirror Telescope, *Orbital Debris Quarterly News*, 2007, April, v11i2,
- [18]Orbital Debris Program Office, Chinese Anti-satellite Test Creates Most Severe Orbital Debris Cloud in History, *Orbital Debris Quarterly News*, 2007, April, v11i2,
- [19]A. MANIS, M. MATNEY, A. VAVRIN, D. GATES, J. SEAGO, P. ANZ-MEADOR, Comparison of the NASA ORDEM 3.1 and ESA MASTER-8 Models, *Orbital Debris Quarterly News*, 2021, Sept, v25i3.

- [20]D. Wright, Space debris, *Physics today*,2007,10,35-40.
- [21]TANG Zhi-mei, DING Zong-hua, DAI Lian-dong, WU Jian, XU Zheng-wen, "The Statistics Analysis of Space Debris in Beam Parking Model in 78° North Latitude Regions," *Space Debris Research*, 2017, 17,3, 1-7.
- [22]TANG Zhimei DING, Zonghua, YANG Song, DAI Liandong, XU Zhengwen, WU Jian The statistics analysis Of space debris in beam parking model based On the Arctic 500 MHz incoherent scattering radar, *CHINESE JOURNAL OF RADIO SCIENCE*, 2018, 25,5, 537-542
- [23]TANG Zhimei, DING, Zonghua, DAI Liandong, WU Jian, XU Zhengwen, Comparative analysis of space debris gaze detection based on the two incoherent scattering radars located at 69N and 78N, *Chin . J . Space Sci*, 2018 38,1, 73-78.
DOI:10.11728/cjss2018.01.073
- [24]DING Zong-hua, YANG Song, JIANG hai, DAI Lian-dong, TANG Zhi-mei, XU Zheng-wen, WU Jian, The Data Analysis of the Space Debris Observation by the Qujing Incoherent Scatter Radar, *Space Debris Research*, 2018, 18,1, 12-19.
- [25]YANG Song, DING Zonghua, Xu Zhengwe, WU Jian, Statistical analysis on the space posture, distribution, and scattering characteristic of debris by incoherent scattering radar in Qujing, *Chinese Journal of Radio science*, 2018 33,6 648-654,
DOI:10.13443/j.cjors.2017112301
- [26]Clet Lab, Clet: a C compiler, download at <https://drive.google.com/file/d/1OjKqANcgZ-9V56rgcoMtOu9w4rP49sgN/view?usp=sharing>
- [27]Huaiyang Cui, Relativistic Matter Wave and Its Explanation to Superconductivity: Based on the Equality Principle, *Modern Physics*, 10,3(2020)35-52. <https://doi.org/10.12677/MP.2020.103005>
- [28]Huaiyang Cui, Relativistic Matter Wave and Quantum Computer, Amazon Kindle ebook, 2021.
- [29]Huaiyang Cui, Evidence of Planck-Constant-Like Constant in Five Planetary Systems and Its Significances, *viXra:2204.0133*, 2022.
- [30]Huaiyang Cui, Approach to enhance quantum gravity effects by ultimate acceleration, *viXra:2205.0053*, 2022.
- [31]N.Cox, *Allen's Astrophysical Quantities*, Springer-Verlag, 2001, 4th ed..
- [32] S. E. Schneider, T. T. Army, *Pathways to Astronomy*, McGraw-Hill Education, 2018, 5th ed.
- [33] https://en.wikipedia.org/wiki/El_Ni%C3%B1o%E2%80%93Southern_Oscillation